Intramolecular Electrostatic Interactions Accelerate Hydrogen Exchange in Diketopiperazine Relative to 2-Piperidone

William R. Forsyth and Andrew D. Robertson*

Contribution from the Department of Biochemistry, University of Iowa, Iowa City, Iowa 52242

Received August 22, 1995[⊗]

Abstract: ^{1}H NMR saturation transfer and T_1 experiments were used to monitor the amide hydrogen exchange rates of 2,5-piperazinedione (diketopiperazine, DKP) and 2-piperidone (δ-valerolactam) in water. Specific acid-catalyzed exchange rate constants (k_H) for δ-valerolactam and DKP are quite similar, but DKP exhibits an approximately 740-fold larger specific base-catalyzed rate constant (k_{OH}) at 25 °C, which approaches the diffusion limit. The rate constants for DKP are larger than expected from simple inductive effects. The enhanced rate constants for DKP are attributed to electrostatic interactions involving the second peptide group. In general, the exchange data and inspection of protein structures suggest that such electrostatic interactions may have significant effects on hydrogen exchange in proteins.

Introduction

Hydrogen exchange has served as a powerful tool for the investigation of protein folding, stability, and function.[1] Numerous labs have demonstrated that hydrogen exchange behaviors of subsets of peptide groups in proteins can provide accurate measures of conformational equilibria in proteins.[2] Interpretation of the hydrogen exchange behavior of peptide groups not reflecting conformational equilibria has been the focus of considerable discussion and is limited by our understanding of the factors that influence hydrogen exchange.[1]

The study of model compounds provides valuable information for the interpretation of hydrogen exchange data.[3−7] Such studies illustrate that inductive effects can modify exchange.[3,4] In linear peptides, electron-withdrawing groups such as peptide groups and various side-chains increase base-catalyzed rate constants up to 100-fold and decrease acid-catalyzed rate constants to a similar extent. On the other hand, electron-donating groups increase acid-catalyzed rate constants and decrease base-catalyzed rate constants.

2-Piperidone (δ-valerolactam, **1**) and 2,5-piperazinedione (diketopiperazine, DKP, **2**) have previously served as model compounds for the study of peptide bond properties.[5] These simple peptides confer the advantage of studying backbone interactions in a relatively rigid structure with an absence of side-chain and end-group effects. In the present study, NMR saturation transfer and T_1 experiments have been used to monitor the amide hydrogen exchange rates of **1** and **2** in water. The rate constants for **2** were found to be significantly enhanced and cannot be explained by simple inductive effects alone. The results suggest that through-space electrostatic interactions are influencing the exchange rates. Similar interactions may affect hydrogen exchange in proteins.

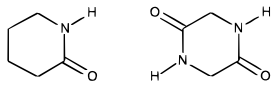

1 **2**

Experimental Section

Materials: Diketopiperazine (glycine anhydride, 99+%) and δ-valerolactam (99+%) were purchased from Aldrich Chemical Co. (Milwaukee, WI). The purity was verified by ^{1}H NMR. TSP (sodium 3-(trimethylsilyl) propionate-2,2,3,3-d_4) and D_2O (99.9 atom %) were from Cambridge Isotope Laboratories (Woburn, MA). Reagent grade potassium chloride, monobasic potassium phosphate, and potassium acetate were from EM Science (Gibbstown, NJ).

NMR Spectroscopy:All samples contained 10 mM DKP or δ-valerolactam, 100 mM potassium chloride, 10 mM monobasic potassium phosphate, 10 mM potassium acetate, 0.89 mM TSP, and 10% D_2O. All water was deionized and distilled. The pH was adjusted with the addition of small amounts of concentrated HCl or KOH. The pH was measured at room temperature using an Orion Research pH meter (Model 611) with a 3 mm o.d. Ingold combination electrode (Wilmad Glass Company; Buena, NJ) standardized at two points with standards

[⊗] Abstract published in *Advance ACS Abstracts,* March 1, 1996.

(1) (a) Bai, Y.; Milne, J. S.; Mayne, L.; Englander, S. W. *Proteins* **1994**, *20*, 4−14. (b) Barksdale, A. D.; Rosenberg, A. *Methods Biochem. Anal.* **1982**, *28*, 1−113. (c) Englander, S. W.; Kallenbach, N. R. *Q. Rev. Biophys.* **1984**, *16*, 521−655. (d) Hvidt, A.; Nielsen, S. O. *Adv. Prot. Chem.* **1966**, *21*, 287−386. (e) Wagner, G.; Wüthrich, K. *Methods Enzymol.* **1986**, *131*, 307−326. (f) Roder, H. *Methods Enzymol.* **1989**, *176*, 446−473. (g) Scholtz, J. M.; Robertson, A. D. Methods in Molecular Biology, Vol 40: Protein Stability and Folding, Theory and Practice, Shirley, B. A., Ed.; Totowa, NJ, 1995; pp 291−311. (h) Woodward, C. K.; Hilton, B. D. *Ann. Rev. Biophys. Bioeng.* **1979**, *8*, 99−127.

(2) (a) Orban, J.; Alexander, P.; Bryan, P.; Khare, D. *Biochemistry* **1995**, *34*, 15291−15300. (b) Perrett, S.; Clarke, J.; Hounslow, A. M.; Fersht, A. R. *Biochemistry* **1995**, *34*, 9288−9298. (c) Wedin, R. E.; Delepierre, M.; Dobson, C. M.; Poulsen, F. M. *Biochemistry* **1982**, *21*, 1098−1103. (d) Swint-Kruse, L,; Robertson, A. D. *Biochemistry* **1996**, *35*, 171−180.

(3) (a) Bai, Y.; Milne, J. S.; Mayne, L.; Englander, S. W. *Proteins* **1993**, *17*, 75−86. (b) Klotz, I. M.; Frank, B. H. *J. Am. Chem. Soc.* **1965**, *87*, 2721−2728. (c) Molday, R. S.; Englander, S. W.; Kallen, R. G. *Biochemistry* **1972**, *11*, 150−158. (d) Sheinblatt, M. *J. Am. Chem. Soc.* **1970**, *92*, 2505−2509.

(4) Molday, R. S.; Kallen, R. G. *J. Am. Chem. Soc.* **1972**, 94, 6739−6745.

(5) (a) Gill, S. J.; Noll, L. *J. Phys. Chem.* **1972**, *76*, 3065−3068. (b) Hooker, T. M., Jr.; Bayley, P. M.; Radding, W.; Schellman, J. A. *Biopolymers* **1974**, *13*, 549−566. (c) Jenkins, G. I.; Taylor, T. W. J. *J. Chem. Soc.* **1937**, 495−497. (d) Murphy, K. P.; Gill, S. J. *J. Chem. Thermodynamics* **1989**, *21*, 903−913. (e) Radding, W.; Donzel, B.; Ueyama, N.; Goodman, M. *J. Am. Chem. Soc.* **1980**, *102*, 5999−6005. (f) Thayer, M. M.; Haltiwanger, R. C.; Allured, V. S.; Gill, S. C.; Gill, S. J. *Biophys. Chem.* **1993**, *46*, 165−169. (g) Susi, H.; Timasheff, S. N.; Ard, J. S. *J. Biol. Chem.* **1964**, *239*, 3051−3054. (h) Tsuboi, M. *Bull. Chem. Soc. Japan* **1949**, *22*, 215−223. (i) Chen, C. Y. S.; Swenson, C. A. *J. Am. Chem. Soc.* **1969**, *91*, 234−237. (j) Gill, S. J.; Hutson, J.; Clopton, J. R.; Downing, M. *J. Phys. Chem.* **1961**, *65*, 1432−1435.

(6) (a) Perrin, C. L.; Johnston, E. R.; Lollo, C. P.; Kobrin, P. A. *J. Am. Chem. Soc.* **1981**, *103*, 4691−4696. (b) Perrin, C. L.; Arrhenius, G. M. L. *J. Am. Chem. Soc.* **1982**, *104*, 6993−6696.

(7) (a) Perrin, C. L.; Lollo, C. P.; Johnston, E. R. *J. Am. Chem. Soc.* **1984**, *106*, 2749−2753. (b) Perrin, C. L.; Johnston, E. R. *J. Am. Chem. Soc.* **1981**, *103*, 4697−4703.

0002-7863/96/1518-2694$12.00/0

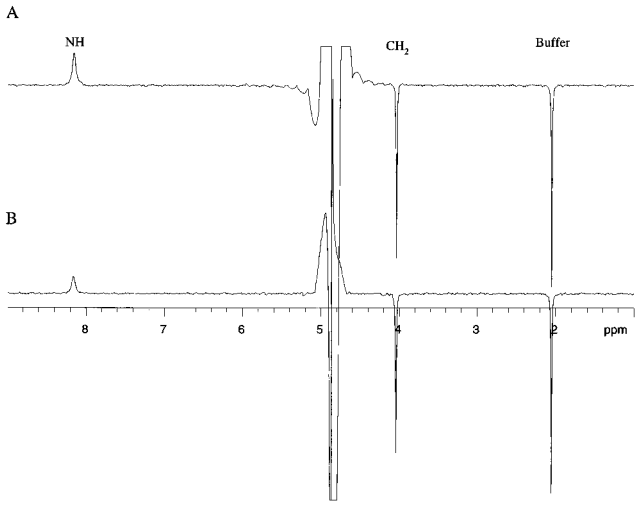

Figure 1. ^{1}H jump-return spectra of 10mM DKP, pH 4.00 at 16 °C. Distortion of the water resonance and the 180° phase shift are artifacts of the pulse sequence. Upper spectrum (A) illustrates the amide intensity in the absence of saturation transfer. Lower spectrum (B) shows a diminished amide intensity due to the transfer of saturation from water. Spectra are normalized according to peak heights of nonexchanging resonances within the range of maximal excitation. The diminished CH_2 resonance (panel B) resulted from poor reproducibility of peak intensity measurements outside the range of maximal excitation.

from VWR Scientific (West Chester, PA) and Fisher Scientific (Pittsburgh, PA). Final sample volumes were 700 μL.

All NMR spectra were recorded using a Nalorac Cryogenics Corporation (Martinez, CA) IDT500 5 mm triple resonance probe on a Varian Unity spectrometer, located in the University of Iowa College of Medicine NMR facility, operating at a ^{1}H frequency of 499.733 MHz. Solvent irradiation was achieved using no more than 35 mW of power for 4 s. Probe temperatures were determined using a methanol standard.[8]

Longitudinal relaxation time constants, T_1, were determined using an inversion-recovery sequence[9] with irradiation of the solvent. Each FID was the sum of eight scans collected as 8000 complex data points and a spectral width of 6000 Hz. The T_1 times were determined in triplicate for each sample.

Fractional amide peak intensities were determined using a $1-\bar{1}$ jump-return pulse sequence in the presence and absence of solvent irradiation.[10] The transmitter was placed at the solvent frequency and the $1-\bar{1}$ delay (~1330 μs for **1** and ~1520 μs for **2**) permitted maximal excitation of the amide proton. Amide peak intensities, measured as peak heights, were normalized to resonance intensities for the nonexchanging protons within the range of maximal excitation. Three determinations were performed for each sample.

The solvent accessible surface area of **2** was calculated based on the Lee and Richards algorithm as implemented in the Insight II program (Release 95.0, BIOSYM/Molecular Simulations, San Diego, CA).[11] Solvent probe radius was 1.4 Å.

Results

pH Dependence of *f* and T_1^{obs}. The transfer of saturation from water to the amide proton is manifested as a diminished amide proton peak intensity in the NMR spectrum (Figure 1). The ratio of the amide proton peak heights in the presence (Figure 1B) and absence of saturation transfer (Figure 1A) describes the fractional peak intensity.

The resulting fractional peak intensity, *f*, depends upon the rate of proton exchange, k_{ex}, and the intrinsic spin-lattice relaxation time constant, T_1^{int}:[12]

$$f = \frac{1}{1 + k_{ex}T_1^{int}} \quad (1)$$

The exchange process also influences the observed T_1, T_1^{obs}, according to:[12]

$$\frac{1}{T_1^{obs}} = \frac{1}{T_1^{int}} + k_{ex} \quad (2)$$

The dependence of k_{ex} on pH can then be analyzed according to

$$k_{ex} = k_H \times 10^{-pH} + k_{OH} \times 10^{(pH-pK_W)} + k_{H_2O} \quad (3)$$

where k_H and k_{OH} are the exchange rate constants for acid- and base-catalysis, respectively. The water ionization constant, pK_W, is corrected for temperature.[13] The pH-independent term, k_{H_2O}, includes the concentration of water.

Amide hydrogen exchange follows pseudo-first-order kinetics, with the observed rates being independent of solute concentration over the ranges of 3−100 mM and 1−100 mM for **1** and **2**, respectively (data not shown). The concentration studies approached the solubility limit of **2** and probably **1**.[5j] The observed independence of hydrogen exchange on solute concentration agrees with the self-association constants for **1** and **2**, 0.013 and 0.018 M^{-1} respectively, which indicate dimer concentrations less than 1% of the total peptide in solution at the highest concentrations.[5d, g]

The pH dependences of *f* and T_1^{obs} for **1** and **2** are shown in Figure 2. The different experimental temperatures of 35 °C for **1** (Figure 2, parts A and C) and 16 °C for **2** (Figures 2B and 2D) were dictated by large differences in hydrogen exchange rates for the two compounds.

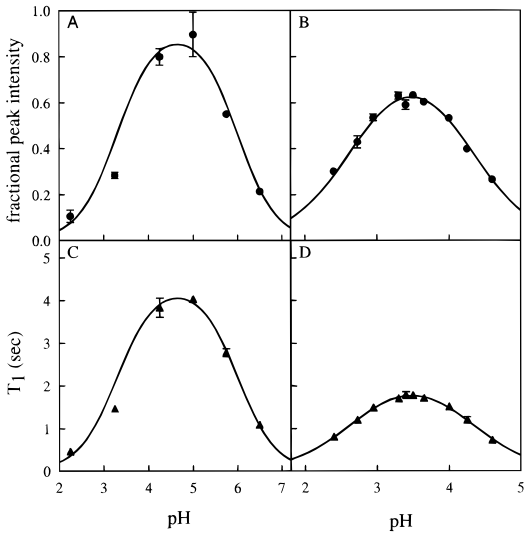

Figure 2. pH dependence of normalized fractional amide intensity (●, A and B) and observed T_1 values (▲, C and D) for δ-valerolactam (A and C, 35.2−36.0 °C) and diketopiperazine (B and D, 16.3−16.8 °C). Lines represent simultaneous nonlinear least-squares fits of the data to eqs 1−3. Error bars, not always visible, represent one standard deviation ($n = 3$).

(8) Van Geet, A. L. *Anal. Chem.* **1968**, *40*, 2227−2229.
(9) Hahn, E. L. *Phys. Rev.* **1949**, *76*, 145−146.
(10) Plateau, P.; Guéron, M. J. Am. Chem. Soc. **1982**, *104*, 7310−7311.
(11) Lee, B.; Richards, F. M. *J. Mol. Biol.* **1971**, *55*, 379−400.
(12) (a) Forsén, S.; Hoffman, R. A. *J. Chem. Phys.* **1964**, *40*, 1189−1196. (b)Forsén, S.; Hoffman, R. A. *J. Chem. Phys.* **1963**, *39*, 2892−2901. (c) O'Neil, J. D. J.; Sykes, B. D. *Biochemistry* **1989**, *28*, 6736−6745.
(13) *Handbook of Chemistry and Physics*, 63rd ed.; Weast, R. C., Astle, M. O., Eds.; Chemical Rubber Publishing Co.: Boca Raton, FL, 1982; p D-174.

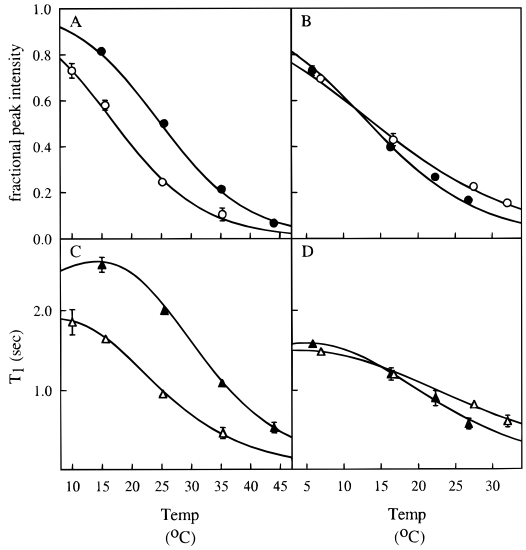

Figure 3. Temperature dependence of normalized fractional amide peak intensities (circles, A and B) and observed T_1 values (triangles, C and D) for δ-valerolactam (A and C) at pH 2.25 (open symbols) and 6.50 (filled symbols) and diketopiperazine (B and D) at pH 2.73 (open symbols) and 4.25 (filled symbols). Lines represent simultaneous nonlinear least-squares fits of the data to eqs 1−2 and 4−5. Error bars, not always visible, represent one standard deviation ($n = 3$).

Activation Energies. Hydrogen exchange was measured at various temperatures to determine the activation energies for acid- and base-catalyzed exchange (Figure 3). While exchange at all pH will have contributions from both of these mechanisms, the experimental pH values were chosen so that one would clearly predominate.

Activation energies for acid- or base-catalysis and the intrinsic relaxation time constant, Ea_k and Ea_{T1} respectively, were obtained by simultaneous fitting of the f and T_1^{obs} data at various temperatures, T, to eqs 1 and 2 and 4 and 5

$$k = k^* \exp\left(\frac{Ea_k}{R}\left(\frac{T - T^*}{T^*T}\right)\right) \tag{4}$$

$$\frac{1}{T_1^{int}} = \frac{1}{T_1^{int*}} \exp\left(\frac{Ea_{T1}}{R}\left(\frac{T - T^*}{T^*T}\right)\right) \tag{5}$$

where R is the gas constant, k^* is the fitted exchange rate constant, and T_1^{int*} is T_1^{int} at the reference temperature, T^*, of 273 K.

The activation energy values for base-catalyzed exchange, corrected for the ionization enthalpy of water, are similar (Table 1).[14,15] However, the activation energy value for acid-catalyzed exchange in **2** is approximately 6 kcal mol^{-1} less than that for **1**. The apparent activation energy values for **1** are in agreement with those reported for linear peptides.[16,17]

The average activation energy for the relaxation rates, 1 / T_1, was 3.6 ± 1.2 kcal mol^{-1} for **1** and 4.6 ± 1.0 kcal mol^{-1} for **2** (data not shown). These values agree with those reported by Rosevear *et al.*, ≤4.2 kcal mol^{-1}, for small peptides.[17]

Hydrogen Exchange Rate Constants. The rate constants reported in Table 2 were obtained by simultaneous fitting of the data in Figure 2 to eqs 1 and 2, substituting eq 3 for k_{ex}, using nonlinear regression.[18] To facilitate comparison of results for **1** and **2**, the activation energy values in Table 1 have been used to calculate rate constants at a common temperature of 25 °C. The k_H values for **1** and **2** are similar, 170 ± 40 and 390 ± 40 M^{-1} s^{-1} respectively. The differences in k_H are statistically significant but negligible compared to the difference in k_{OH}: the extrapolated k_{OH} value for **2** is (5.8 ± 0.8) × 10^9 M^{-1} s^{-1}, about 740-fold larger than the (7.9 ± 1.2) × 10^6 M^{-1}s^{-1} for **1** at 25 °C . The rate constant for **2** thus approaches the diffusion limit.[19] The rate constants for **1** are in good agreement with the hydrogen−deuterium rate constants reported by Chen and Swenson[5i] at 24.9 °C, k_D = 267 ± 7 M^{-1} s^{-1} and k_{OD} = (4.63 ± 0.10) × 10^6 M^{-1} s^{-1}.

Table 1. Summary of Amide Activation Energies

	pH	Ea (kcal mol^{-1})[a]	temp (°C)[b]
δ-valerolactam	2.25	18 (2)	10.0−35.3
	6.50	6 (1)	15.0−44.0
diketopiperazine	2.73	12 (1)	6.9−32.1
	4.25	3 (2)	5.8−26.8

[a] The data in Figure 3 were fit simultaneously to eq 1 and 2 and 4 and 5 using nonlinear regression to determine the apparent activation energies. Numbers in parentheses represent errors of the fits at one standard deviation. [b] Temperature range over which data were collected.

Discussion and Conclusions

Amide hydrogen exchange rates are modulated by substituents.[3,4] In derivatives of *N*-methylacetamide, k_{OH} increases 4-fold upon the addition of a peptide group on the carbonyl side, while replacement of the methyl with a peptidyl substituent on the nitrogen increases k_{OH} approximately 17-fold.[4] These nearest neighbor inductive effects are additive.[1a, 3c] The observed 740-fold increase in k_{OH} in **2** relative to **1** thus suggests that the additional peptide bond in **2** is exerting more than a simple inductive effect on exchange.

Inspection of the crystal structure of **2** reveals that only 2.5 Å separates the nitrogen of one peptide group from the carbonyl carbon of the second peptide group. The overlapping van der Waals radii suggests the possibility of a significant electrostatic interaction between atoms of the two peptide groups.[20]

Electrostatic calculations based on Coulomb's law were used to estimate relative magnitudes of the interactions between the peptide groups in **2** (Table 3). Atoms were treated as point charges and one dielectric constant was used for both the compound and solvent. The use of a single dielectric probably leads to an underestimation of the interaction energies among the amide nitrogens and carbonyl carbons relative to interactions involving the carbonyl oxygens and amide hydrogens, which are more solvated than the ring atoms (Table 3).

Distances measured from the crystal structure of **2** were used to calculate the electrostatic free energy of interaction, G_{el}, according to

$$G_{el} = \frac{q_1 q_2}{4\pi\epsilon_o \epsilon r} \tag{6}$$

where q is the atomic charges of the interacting atoms separated by a distance r, ϵ_o is the permittivity of a vacuum (2.116 ×

(14) Hvidt, A.; Gesmar, H.; Led, J. J. *Acta Chem. Scan. B* **1983**, *37*, 227−234.
(15) Fasman, G. D. Handbook of Biochemistry and Molecular Biology: Physical and Chemical Data, Volume 1, 3rd ed.; Chemical Rubber Co.: Cleveland, OH, 1976; pp 260−261.
(16) Leichtling, B. H.; Klotz, I. M. *Biochemistry* **1966**, *5*, 4026−4037.
(17) Rosevear, P. R.; Fry, D. C.; Mildvan, A. S. *J. Magn. Reson.* **1985**, *61*, 102−115.
(18) (a) Johnson, M. L.; Faunt, L. M. *Methods Enzymol.* **1992**, *210*, 1−37. (b) Johnson, M. L.; Frasier, S. G. *Methods Enzymol.* **1985**, *117*, 301−342.
(19) Eigen, M. *Agnew. Chem., Int. Ed. Engl.* **1964**, *3*, 1−72.
(20) (a) Bondi, A. *J. Phys. Chem.* **1964**, *68*, 441−451. (b) Eisenberg, D.; Crothers, D. Physical Chemistry with Applications to the Life Sciences, Benjamin/Cummings Publishing Company, Inc.: Menlo Park, CA, 1979; pp 503−508.

Table 2. Summary of Hydrogen Exchange Rate Measurements[a]

	temp (°C)	k_H (10^{-2} M^{-1} s^{-1})	k_{OH} (10^{-7} M^{-1} s^{-1})	k_{H_2O} (10^2 s^{-1})	T_1^{int} [b](s)
δ-valerolactam	35	4.5 (0.5)	1.1 (0.1)	1.6 (1.8)	4.8 (0.4)
	25[c]	1.7 (0.4)	0.79 (0.12)		3.8 (0.7)
diketopiperazine	16	2.0 (0.1)	500 (20)	7.7 (1.5)	2.8 (0.1)
	25[c]	3.9 (0.4)	580 (80)		3.6 (0.3)

[a] The data in Figure 2 were fit simultaneously to eqs 1−3 using nonlinear regression to determine the catalytic rate constants. Values in parentheses represent errors of the fits at one standard deviation. [b] The fitted values of the intrinsic T_1 for the exchanging amides. [c] Extrapolated rate constants based on the experimentally determined apparent activation energies reported in Table 1.

Table 3. Calculated Electrostatic Free Energies of Interaction in Diketopiperazine

	distance (Å)[a]	atomic charge (1.602×10^{19} C)[b]	G_{el} (kcal mol^{-1})[c]	SAS area (Å^2)[d]
		Amide Nitrogen[e]		
N	2.8	−0.20	2.4	5.4
H	3.6	0.20	−1.8	23.3
C	2.5	0.42	−5.6	7.8
O	3.6	−0.42	3.9	41.9
		Carbonyl Oxygen[f]		
N	3.6	−0.20	3.9	5.4
H	4.3	0.20	−3.2	23.3
C	4.1	0.42	−7.1	7.8
O	5.3	−0.42	5.5	41.9

[a] Distances determined from the crystal structure.[21] [b] Typical atomic charges for peptide atoms.[22] The use of partial atomic charges based on semiemperical and *ab initio* calculations alters the absolute but not relative magnitudes of the free energies of interaction.[23] [c] Electrostatic free energies based on eq 6 and a dielectric constant of 2. Negative values indicate favorable interactions. [d] Mean solvent accessible surface area for peptide atom.[11] [e] Interactions between an amide nitrogen and atoms of the second peptide group. N, H, C, and O signify the amide nitrogen, amide hydrogen, carbonyl carbon, and carbonyl oxygen of the second peptide group. [f] Interactions between a carbonyl oxygen and atoms of the second peptide group.

Scheme 1

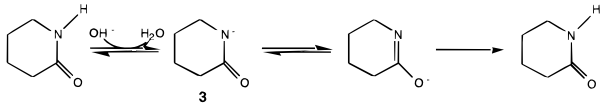

3

10^{-9} $kcal^{-1}$ C^2 m^{-1}), and ϵ is the effective dielectric constant.[24] The choice of a dielectric constant, which is 2 for the present calculations, is somewhat arbitrary in that our aim is a semiquantitative evaluation of interactions present in **2** but not in **1**.

The calculations suggest a relatively strong favorable interaction between the amide nitrogen and carbonyl carbon of the two peptide groups (Table 3). While several unfavorable interactions with the carbonyl oxygen are indicated, the calculations ignore the increased solvent accessibility of this atom. Any correction for solvent accessibility would only increase the amide nitrogen−carbonyl carbon interaction and attenuate the other interactions.

The significance of the electrostatic interactions may be interpreted in terms of the exchange mechanisms. For both compounds, base-catalyzed exchange involves direct deprotonation of the nitrogen (Scheme 1).[3d,6,16] The rate-determining step in base-catalyzed exchange is deprotonation of the amide

Scheme 2

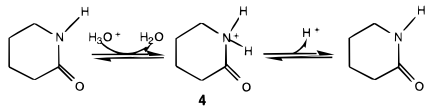

4

Scheme 3

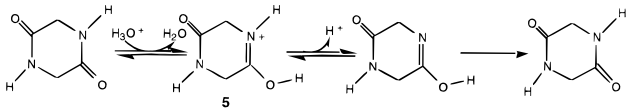

5

to form anion **3**.[3d, 6, 16] During base-catalysis, the increased negative charge of the deprotonated nitrogen will interact more favorably with the carbonyl carbon of the second peptide group in **2**, thereby accelerating the exchange rate.

The presence of the second peptide group in **2** alters the mechanism of acid-catalyzed exchange.[6] While **1** exchanges primarily through the N-protonation mechanism (Scheme 2), the additional electron-withdrawing peptide group in **2** promotes the imidic acid mechanism (Scheme 3). The rate-determining step for acid-catalyzed exchange is deprotonation of cations **4** and **5**, with the overall rate being the product of this step and the preceding equilibrium.[7]

Two electrostatic interactions may be involved in the enhanced acid-catalyzed rate constant of **2**. First, the favorable interaction between an amide nitrogen of one peptide group with the carbonyl carbon of the other peptide may polarize the carbonyl bond thereby promoting the initial protonation of the carbonyl oxygen (Scheme 3). The electrostatic calculations further suggest that a destabilizing interaction may arise between the protonated nitrogen and the carbonyl carbon of the other peptide group thus facilitating deprotonation of cation **5**. The effects of the second peptide group in **2** on the equilibrium leading to **5** are unclear.

In **2**, both k_H and k_{OH} are increased about 10-fold beyond the expected inductive effects. The electrostatic calculations are consistent with the observed rate enhancements in **2** relative to **1**. Further evidence for changes in amide acidity is the enhanced hydrolysis rates of the peptide bonds in **2** with respect to linear di- and tripeptides.[25] In addition, the amide proton resonance for **2** is shifted downfield about 0.7 ppm relative to **1**, which is consistent with an increase in the acidity of **2** (data not shown).[4]

Through-space electrostatic interactions have been hypothesized to alter hydrogen exchange rates in peptides and proteins.[26] The altered rates can result from several mechanisms. First, the electrostatic field may alter the local pH at the exchangeable site: a region with a high charge density will

(21) Degeilh, R.; Marsh, R. E. *Acta Crystallogr*. **1959**, *12*, 1007−1014.
(22) (a) Creighton, T. E. Proteins: Structures and Molecular Properties, 2nd ed., W. H. Freeman and Company: New York, NY, 1993; p 145. (b) Avbelj, F.; Moult, J. *Biochemistry* **1995**, *34*, 755−764. (c) Yan, J. F.; Momany, F. A.; Hoffmann, R.; Sheraga, H. A. *J. Phys. Chem.* **1970**, *74*, 420−433.
(23) Hagler, A. T.; Lapiccirella, A. *Biopolymers*, **1976**, *15*, 1167−1200.
(24) Eisenberg, D; Crothers, D. Physical Chemistry with Applications to the Life Sciences, Benjamin/Cummings Publishing Company, Inc.: Menlo Park, CA, 1979; pp 331−342.
(25) Sykes, B. D.; Robertson. E. B.; Dunford, H. B.; Konasewich, D. *Biochemistry* **1966**, *5*, 697−701.
(26) (a) Kim. P. S.; Baldwin, R. L. *Biochemistry* **1982**, *21*, 1−5. (b) Matthew, J. B.; Richards, F. M. *J. Biol. Chem.* **1983**, *258*, 3039−3044. (c) Dempsey, C. E. *J. Am. Chem. Soc.* **1995**, *117*, 7526−7534. (d) Dempsey, C. E. *Biochemistry* **1988**, *27*, 6983−6901. (e) Dempsey, C. E. *Biochemistry* **1986**, *25*, 3904−3911. (f) Rohl, C. A.; Baldwin, R. L. *Biochemistry* **1994**, *33*, 7760−7767. (g) Eriksson, M. A. L.; Härd, T.; Nilsson, L. *Biophys. J.* **1995**, *69*, 329−339.

be surrounded by counterions thereby altering the local pH and, hence, the exchange rate. This counterion condensation mechanism was used to explain the ionic strength dependence of amide hydrogen exchange rates from the neutral poly(DL-alanine) and the positively charged poly(DL-lysine) polypeptides.[26a] Another mechanism of altering exchange rates is through the burial of ionizable groups in a protein structure thereby inhibiting interactions with catalyst. Additionally, when ionized, a residue may interact with dipoles or other charged residues. Such electrostatic interactions may alter the effective acidity or pK_a of the ionizable group as in the case with **2**.

The proposed interactions responsible for the enhanced hydrogen exchange rate of **2** span very short distances (Table 3). Similarly short distances among neutral polar groups are also found in regions of secondary structure in proteins.[27] Interpeptide carbonyl carbon to carbonyl oxygen distances in regions of β-sheet in p21^{ras} were found to range from 3.5 to 7.9 Å, while α-carbon(i) to α-carbon(i+3) distances for strict type I β turns are 4.6 Å.[27d,e] The proximity of uncharged polar groups has been proposed to cause the enhanced hydrogen exchange rates observed for some peptide groups in proteins.[2a−c]

A recent study reporting hydrogen exchange data for the B1 domain of protein G found that the backbone amides of Lys 10, Thr 11, and Leu 12 had exchange rates five- to 24-fold larger than the corresponding model peptides at pD 3.1.[2a] These residues are located in a type I β turn between the first and second β-strands with the amides aligned in the same direction.[28] The authors propose that the resulting local positive electrostatic field may lead to counterion condensation of hydroxide ions around that region which would enhance base-catalysis. Alternatively, the proximity of the positive amide hydrogens may also serve to stabilize anion **3** during base-catalysis, thereby enhancing the exchange rates.

Rapid hydrogen exchange rates for several buried amides in bovine pancreatic trypsin inhibitor, BPTI, have been attributed to electrostatic influences.[29] Inspection of a BPTI crystal structure revealed that some of the backbone amides, such as that of Asp 50, were located at the N-terminus of a helix.[30] The authors propose that the positive potential generated at the N-terminus of the helix not only increased the local hydroxide ion concentration but also stabilized the negative charge on the deprotonated intermediate **3** (Scheme 1), thereby promoting amide deprotonation and increasing base catalysis. They also propose that the low k_H for Asp 50 resulted from electrostatic interactions with the helix dipole which inhibited acid-catalysis through cation repulsion and destabilized the positively charged intermediate **5** (Scheme 3).

Numerous other studies have illustrated the possible influence of a helix dipole on acidity, hence hydrogen exchange rates.[26c−f,31] For instance, the amides at the termini of the alamethicin helix exhibited exchange constants which were altered up to 20-fold relative to model peptides with the same nearest neighboring amino acid side chains.[26c] The helix dipole is attributed with enhancing k_{OH} for the non-hydrogen bonded N-terminal residue while increasing k_H for the hydrogen bonded C-terminal residues. Similar enhancements of k_{OH} for N-terminal residues have been reported for other helical peptides such as melittin, apamin, and some alanine based peptides.[26d−f]

Other implications of backbone electrostatic interactions have been the focus of several recent studies. Maccallum *et al.*,[32] have proposed that such backbone interactions may play an important role in stabilizing regions of secondary structure, especially β-sheets. Such interactions have also been proposed to contribute to the conformational preference of amino acid residues.[22b] Hence, interactions among neutral polar backbone atoms may have far reaching consequences on protein structure, stability, and function. The present study illustrates the potential magnitude of the effect of one neutral polar group on the reactivity of nearby peptide groups.

Acknowledgment. We are grateful to Dr. C. L. Perrin for his comments and to Dr. M. K. Gilson for his advice on the electrostatic calculations. This work was supported by the National Institutes of Health (GM 46869 to A.D.R.). We dedicate this paper to Professor Charles A. Swenson on the occasion of his retirement.

JA952892M

(27) (a) Kabsch, W.; Sander, C. *Biopolymers* **1983**, *22*, 2577−2637. (b) Baker, E. N.; Hubbard, R. E. *Prog. Biophys. Mol. Biol.* **1984**, *44*, 97−179. (c) Barlow, D. J.; Thornton, J. M. *J. Mol. Biol.* **1988**, *201*, 601−619. (d) Rose, G. D. *Adv. Protein Chem.* **1985**, *37*, 1−109. (e) Maccallum, P. H.; Poet, R.; Milner-White, E. J. *J. Mol. Biol.* **1995**, *248*, 361−373.

(28) (a) Gallagher, T.; Alexander, P.; Bryan, P.; Gilliland, G. L. *Biochemistry* **1994**, *33*, 4721−4729. (b) Gronenborn, A. M.; Filpula, D. R.; Essig, N. Z.; Achari, A.; Whitlow, M.; Wingfield, P. T.; Clore, G. M. *Science* **1991**, *253*, 657−661.

(29) (a) Tüchsen, E.; Woodward, C. *J. Mol. Biol.* **1985**, *185*, 405−419. (b) Tüchsen, E.; Woodward, C. *J. Mol. Biol.* **1985**, *185*, 421−430.

(30) Wlodawer, A.; Nachman, J.; Gilliland, G. L.; Gallagher, W.; Woodward, C. J. *J. Mol. Biol.* **1987**, *198*, 469−480.

(31) (a) Kortemme, T.; Creighton, T. E. *J. Mol. Biol.* **1995**, *253*, 799−812. (b) Walter, S.; Hubner, B.; Ulrich, H.; Schmid, F. X. *J. Mol. Biol.* **1995**, *252*, 133−143.

(32) (b) Maccallum, P. H.; Poet, R.; Milner-White, E. J. *J. Mol. Biol.* **1995**, *248*, 374−384.